

COMPOSITE SPIN AND QUADRUPOLE WAVE IN THE ORDERED PHASE OF $\text{Tb}_{2+x}\text{Ti}_{2-x}\text{O}_{7+y}$

H. Kadowaki

Department of Physics, Tokyo Metropolitan University, Hachioji-shi, Tokyo 192-0397, Japan

H. Takatsu

Department of Physics, Tokyo Metropolitan University, Hachioji-shi, Tokyo 192-0397, Japan

T. Taniguchi

Department of Physics, Tokyo Metropolitan University, Hachioji-shi, Tokyo 192-0397, Japan

B. Fåk

Institute Laue Langevin, BP156, F-38042 Grenoble, France

J. Ollivier

Institute Laue Langevin, BP156, F-38042 Grenoble, France

Received 30 April 2015

The hidden ordered state of the frustrated pyrochlore oxide $\text{Tb}_{2+x}\text{Ti}_{2-x}\text{O}_{7+y}$ is possibly one of the two electric multipolar, or quadrupolar, states of the effective pseudospin-1/2 Hamiltonian derived from crystal-field ground state doublets of non-Kramers Tb^{3+} ions. These long-range orders are antiparallel or parallel alignments of transverse pseudospin components representing electric quadrupole moments, which cannot be observed as magnetic Bragg reflections by neutron scattering. However pseudospin waves of these states are composite waves of the magnetic-dipole and electric-quadrupole moments, and can be partly observed by inelastic magnetic neutron scattering. We calculate these spin-quadrupole waves using linear spin-wave theory and discuss previously observed low-energy magnetic excitation spectra of a polycrystalline sample with $x = 0.005$ ($T_c = 0.5$ K).

Keywords: frustration, pyrochlore, magnon

1. Introduction

Geometrically frustrated magnets have been actively studied in recent years¹. In particular, pyrochlore magnets² showing spin ice behavior³ have interesting features such as finite zero-point entropy and emergent magnetic monopole excitations⁴. A quantum spin-liquid state is theoretically predicted for certain spin-ice like systems^{5; 6; 7; 8; 9}, where transverse spin interactions transform the classical spin ice into quantum spin liquid. This quan-

tum spin ice (QSI), or U(1) quantum spin liquid, is characterized by an emergent U(1) gauge field fluctuating down to $T = 0$ and by excitations of gapped bosonic spinons and gapless photons^{5; 7; 10}. By changing the interactions of the QSI in some ways the system undergoes a quantum phase transition to long range ordered (LRO) states of transverse spin or pseudospin⁶, being interpreted as Higgs phases^{7; 11}. Experimental investigations of the U(1) quantum spin liquid and neigh-

boring LRO states have been challenged by several groups^{11; 12; 9}. However it is difficult to characterize the quantum spin liquid states, which preclude standard techniques of observing magnetic Bragg reflections and magnons.

Among magnetic pyrochlore oxides², $R_2Ti_2O_7$ ($R = Dy, Ho$) are the well-known classical Ising spin-ice examples³. A similar system $Tb_2Ti_2O_7$ (TTO) has attracted much attention, because magnetic moments remain dynamic with short range correlations down to 50 mK¹³. Since TTO has been thought to be close to the classical spin ice, the low-temperature dynamical behavior of TTO could be attributed to QSI¹⁴. Inspired by this intriguing idea, many experimental studies of TTO have been performed to date^{15; 16; 17; 18; 19; 20} (and references in Refs. 9 and 21). However the interpretation of experimental data has been a conundrum^{9; 21}, partly owing to strong sample dependence^{22; 15; 16}. Among these studies, our investigation¹⁶ of polycrystalline $Tb_{2+x}Ti_{2-x}O_{7+y}$ showed that a very small change of x induces a quantum phase transition between a spin-liquid state ($x < -0.0025 = x_c$) and a LRO state with a hidden order parameter ($x_c < x$). It is important to clarify the origin of this order parameter, which becomes dynamical in the spin-liquid state ($x < x_c$).

In this and companion²³ work, we try to reformulate the problem of TTO and to reinterpret its puzzling experimental data based on the theoretically predicted²⁴ electronic superexchange interactions. A novel ingredient of these interactions is the Onoda-type coupling²⁴ between neighboring electric quadrupole moments of non-Kramers Tb^{3+} ions. The theory²⁴ proposes an effective pseudospin-1/2 Hamiltonian described by the Pauli matrices representing both magnetic-dipole and electric-quadrupole moments. Depending on the parameters of the Hamiltonian there are two electric quadrupole ordering phases, which are candidates for the hidden order of TTO. These electric quadrupolar orders do not bring about observable magnetic Bragg peaks. However, these orders can be detected by their elementary excitations (inelastic magnetic scattering), and by proper interpretation using a linear spin-wave theory.

In this paper, starting from the crystal-field (CF) ground state doublet of TTO, we account for its single-site electric quadrupole moments,

their LRO, and pseudospin wave excitations in the electric quadrupole LRO. A standard linear spin-wave theory predicts that the pseudospin wave in the electric quadrupole LRO is, in reality, a composite wave of magnetic-dipole and electric-quadrupole moments. We discuss this possibility for $Tb_{2+x}Ti_{2-x}O_{7+y}$ using previously observed¹⁶ low-energy magnetic excitation spectra of a polycrystalline sample with $x = 0.005$ ($T_c = 0.5$ K).

2. Crystal Field and Electric Multipole Moment

The CF states and inelastic neutron excitation spectra of TTO have been investigated by many authors^{25; 26; 27; 28; 29}; readers are referred to Ref. 29 for details. In a low energy range, there are four CF states: ground doublet states and first-excited doublet states at $E \sim 16$ K. Since the interesting temperature range is below 1 K, we neglect the first-excited doublet states and consider only the ground state doublet, for simplicity.

Among studies of CF, we adopt the CF parameters of Ref. 26 (or Ref. 27). The CF ground state doublet of TTO can be written by

$$|\pm 1\rangle_D = A|\pm 4\rangle \mp B|\pm 1\rangle + C|\mp 2\rangle \pm D|\mp 5\rangle, \quad (1)$$

where $|m\rangle$ stands for the $|J = 6, m\rangle$ state within a JLS -multiplet³⁰. The coefficients²⁶ of Eq. (1) are $A = 0.9581$, $B = 0.1284$, $C = 0.1210$, $D = 0.2256$. The local symmetry axes^{27; 24} of the crystallographic four sites are

$$\mathbf{x}_0 = \frac{1}{\sqrt{6}}(1, 1, \bar{2}), \mathbf{y}_0 = \frac{1}{\sqrt{2}}(\bar{1}, 1, 0), \mathbf{z}_0 = \frac{1}{\sqrt{3}}(1, 1, 1) \quad (2)$$

for sites at $\mathbf{t}_n + \mathbf{d}_0$ with $\mathbf{d}_0 = \frac{1}{4}(0, 0, 0)$,

$$\mathbf{x}_1 = \frac{1}{\sqrt{6}}(1, \bar{1}, 2), \mathbf{y}_1 = \frac{1}{\sqrt{2}}(\bar{1}, \bar{1}, 0), \mathbf{z}_1 = \frac{1}{\sqrt{3}}(1, \bar{1}, \bar{1}) \quad (3)$$

for sites at $\mathbf{t}_n + \mathbf{d}_1$ with $\mathbf{d}_1 = \frac{1}{4}(0, 1, 1)$,

$$\mathbf{x}_2 = \frac{1}{\sqrt{6}}(\bar{1}, 1, 2), \mathbf{y}_2 = \frac{1}{\sqrt{2}}(1, 1, 0), \mathbf{z}_2 = \frac{1}{\sqrt{3}}(\bar{1}, 1, \bar{1}) \quad (4)$$

for sites at $\mathbf{t}_n + \mathbf{d}_2$ with $\mathbf{d}_2 = \frac{1}{4}(1, 0, 1)$,

$$\mathbf{x}_3 = \frac{1}{\sqrt{6}}(\bar{1}, \bar{1}, \bar{2}), \mathbf{y}_3 = \frac{1}{\sqrt{2}}(1, \bar{1}, 0), \mathbf{z}_3 = \frac{1}{\sqrt{3}}(\bar{1}, \bar{1}, 1) \quad (5)$$

for sites at $\mathbf{t}_n + \mathbf{d}_3$ with $\mathbf{d}_3 = \frac{1}{4}(1, 1, 0)$, where \mathbf{t}_n is an FCC translation vector.

In the CF ground state doublet of Eq. (1), the magnetic-dipole and electric-multipole moment operators³¹ are represented by 2×2 matrices: the Pauli matrices σ^x , σ^y , σ^z and the unit matrix. The magnetic dipole moment operators within $|\pm 1\rangle_D$

are

$$J_x = J_y = 0, \\ J_z = (4A^2 + B^2 - 2C^2 - 5D^2)\sigma^z = 3.40\sigma^z, \quad (6)$$

which implies that Tb^{3+} magnetic dipole moments behave as Ising-like spins.

As pointed out in Ref. 24, for non-Kramers ions in the pyrochlore structure including Tb^{3+} in TTO the CF ground doublet states have additionally electric multipole moments. These electric multipole moment operators are represented by σ^x , σ^y , and the unit matrix. Using the explicit form of Eq. (1), the electric quadrupole moment operators³¹ within $|\pm 1\rangle_{\text{D}}$ are expressed by

$$\begin{aligned} \frac{1}{2}[3J_z^2 - J(J+1)] &= 3A^2 - \frac{39}{2}B^2 - 15C^2 + \frac{33}{2}D^2 \\ &= 3.05, \\ \frac{\sqrt{3}}{2}[J_x^2 - J_y^2] &= \left(-\frac{21\sqrt{3}}{2}B^2 + 9\sqrt{10}AC\right)\sigma^x \\ &= 3.00\sigma^x, \\ \frac{\sqrt{3}}{2}[J_xJ_y + J_yJ_x] &= \left(-\frac{21\sqrt{3}}{2}B^2 + 9\sqrt{10}AC\right)\sigma^y \\ &= 3.00\sigma^y, \\ \frac{\sqrt{3}}{2}[J_zJ_x + J_xJ_z] &= \left(-3\sqrt{30}BC - 9\sqrt{\frac{33}{2}}AD\right)\sigma^x \\ &= -8.16\sigma^x, \\ \frac{\sqrt{3}}{2}[J_yJ_z + J_zJ_y] &= \left(3\sqrt{30}BC + 9\sqrt{\frac{33}{2}}AD\right)\sigma^y \\ &= 8.16\sigma^y. \end{aligned} \quad (7)$$

Similarly we can show that the electric 16-pole and 64-pole moment operators³¹, expressed by the Racah operators³⁰ $\tilde{O}_{p,q}(\mathbf{J})$ with $p = 4$ and 6 , respectively (or Stevens's operators), are proportional to $\sigma^x \pm i\sigma^y$ or the unit matrix within $|\pm 1\rangle_{\text{D}}$. Therefore within the CF ground state doublet, pseudospin operators σ^x and σ^y represent the electric multipole moments. A single-site CF ground state expressed by

$$|\psi\rangle = (|1\rangle_{\text{D}}, |-1\rangle_{\text{D}})\chi, \quad (8)$$

where χ is the pseudospin wave-function, has the largest expectation of the magnetic dipole moment $|\langle\psi|\sigma^z|\psi\rangle| = 1$ (and $\langle\psi|\sigma^x|\psi\rangle = \langle\psi|\sigma^y|\psi\rangle = 0$) for $\chi = \begin{pmatrix} 1 \\ 0 \end{pmatrix}$ or $\chi = \begin{pmatrix} 0 \\ 1 \end{pmatrix}$. The other states expressed by

$$\chi = \begin{pmatrix} \cos\frac{\theta}{2}e^{-i\phi/2} \\ \sin\frac{\theta}{2}e^{i\phi/2} \end{pmatrix} \quad (9)$$

in which θ is in the range $0 < \theta < \pi$ have finite expectation values of the electric quadrupole moment operators; $\langle\psi|\sigma^x|\psi\rangle \neq 0$ and/or $\langle\psi|\sigma^y|\psi\rangle \neq$

0. These states have slightly deformed f -electron charge densities from that of the magnetic states with $\theta = 0$ or $\theta = \pi$. More specifically, the approximate f -electron charge density³¹ of the state $|\psi\rangle$ is given by

$$\langle\psi|\rho(\mathbf{r})|\psi\rangle \simeq (-e)[R_f(r)]^2\langle\psi|\rho_e(\hat{\mathbf{r}})|\psi\rangle\frac{1}{4\pi}. \quad (10)$$

The angular dependence³¹ $\rho_e(\hat{\mathbf{r}})$ of this equation is

$$\rho_e(\hat{\mathbf{r}}) = n + \sum_{p=2,4,6;q} [4\pi(2p+1)]^{1/2}\alpha_p Y_{p,q}(\hat{\mathbf{r}})^* \tilde{O}_{p,q}(\mathbf{J}), \quad (11)$$

where $(\alpha_2, \alpha_4, \alpha_6) = (\alpha, \beta, \gamma)$ are the Stevens factors³⁰, $n = 8$ is the number of f -electrons, and $Y_{p,q}(\hat{\mathbf{r}})$ are the spherical harmonics. By evaluating $\langle\psi|\rho_e(\hat{\mathbf{r}})|\psi\rangle$ using several spinors of Eq. (9), one can show that the deformation of the f -electron charge density is mainly determined by the electric quadrupole moments. The electric 16-pole and 64-pole moments have non-negligible contributions to the deformation similarly to the analyses of the CF states^{25; 26; 27; 28; 29}. In these meanings, the CF ground (pseudospin-1/2) states $|\psi\rangle$ can be referred to as composite spin and quadrupole states.

3. Effective Pseudospin-1/2 Hamiltonian

The generic form of the effective pseudospin-1/2 Hamiltonian for non-Kramers CF ground state doublets of $4f$ magnetic ions in the pyrochlore structure was derived in Ref. 24 by calculating the nearest-neighbor (NN) superexchange interaction. This Hamiltonian consists of two parts. The first part is the NN magnetic interaction

$$H_{\text{m,NN}} = J_{\text{nn}} \sum_{\langle\mathbf{r},\mathbf{r}'\rangle} \sigma_{\mathbf{r}}^z \sigma_{\mathbf{r}'}^z, \quad (12)$$

which represents the NN classical spin-ice model for $J_{\text{nn}} > 0$. The second part is the NN quadrupolar interaction

$$\begin{aligned} H_{\text{q}} &= J_{\text{nn}} \sum_{\langle\mathbf{r},\mathbf{r}'\rangle} [2\delta(\sigma_{\mathbf{r}}^+ \sigma_{\mathbf{r}'}^- + \sigma_{\mathbf{r}}^- \sigma_{\mathbf{r}'}^+) \\ &\quad + 2q(e^{2i\phi_{\mathbf{r},\mathbf{r}'}} \sigma_{\mathbf{r}}^+ \sigma_{\mathbf{r}'}^+ + \text{H.c.})], \end{aligned} \quad (13)$$

where $\sigma_{\mathbf{r}}^{\pm} = (\sigma_{\mathbf{r}}^x \pm i\sigma_{\mathbf{r}}^y)/2$ and $\sigma_{\mathbf{r}}^{\alpha}$ ($\alpha = x, y, z$ defined using the local axes Eqs. (2)-(5)) stand for the Pauli matrices of the pseudospin at a site \mathbf{r} . The phases $\phi_{\mathbf{r},\mathbf{r}'}$ are $\phi_{\mathbf{r},\mathbf{r}'} = 0, -2\pi/3, \text{ and } 2\pi/3$ for $(i, i') = (0, 3), (1, 2), (i, i') = (0, 1), (2, 3), \text{ and } (i, i') = (0, 2), (1, 3)$, respectively, where $(\mathbf{r}, \mathbf{r}') = (\mathbf{t}_n + \mathbf{d}_i, \mathbf{t}_{n'} + \mathbf{d}_{i'})$.

For the magnetic interaction of TTO we probably have to include the classical dipolar interaction, i.e.,

$$H_m = H_{m,NN} + Dr_{nn}^3 \times \sum_{\langle r,r' \rangle} \left\{ \frac{\mathbf{z}_r \cdot \mathbf{z}_{r'}}{|\Delta \mathbf{r}|^3} - \frac{3[\mathbf{z}_r \cdot \Delta \mathbf{r}][\mathbf{z}_{r'} \cdot \Delta \mathbf{r}]}{|\Delta \mathbf{r}|^5} \right\} \sigma_r^z \sigma_{r'}^z \quad (14)$$

where the summation runs over all pairs of sites, r_{nn} is the NN distance, and $\Delta \mathbf{r} = \mathbf{r} - \mathbf{r}'$. The parameter D is determined by the magnetic moment of the CF ground state doublet. We adopt $D = 0.29$ K, corresponding to the experimental value of the magnetic moment $4.6 \mu_B$ ²³. As discussed in Refs. 32 and 33, when the magnetic interaction of Eq. (14) represents the dipolar spin ice ($J_{nn} + D_{nn} > 0$), H_m can be approximated by the NN classical spin-ice Hamiltonian³²

$$H_m \simeq (J_{nn} + D_{nn}) \sum_{\langle r,r' \rangle} \sigma_r^z \sigma_{r'}^z, \quad (15)$$

where $D_{nn} = \frac{5}{3}D = 0.48$ K.

In our computations we used an effective pseudospin-1/2 Hamiltonian of the form

$$H_{\text{eff}} = H_m + H_q. \quad (16)$$

We note that this is not very different from the original Onoda-type interaction²⁴ ($D_{nn} = 0$) and results of Refs. 24 and 7 can be approximately used at least in the electric quadrupolar phases, in which xy -components of the pseudospin (σ_r^x, σ_r^y) show LRO and semi-classical theoretical treatments are applicable.

4. Pseudospin Wave

The studies^{24; 7; 23} of the effective Hamiltonian of Eq. (16) showed that there are two electric quadrupolar states: the PAF state (planar antiferropseudospin) and the PF state (planar ferropseudospin) depending on the two parameters (δ, q) (see Fig. 7 in Ref. 24 and Fig. 3 in Ref. 7 for details). In these states, the xy -components of the pseudospin show LRO with the modulation vector $\mathbf{k} = 0$. It should be noted that this wave vector $\mathbf{k} = 0$ is selected by quantum⁷ and thermal^{24; 23} fluctuations for PAF, i.e., by an order-by-disorder mechanism.

In order to calculate elementary excitations in the PAF and PF states, we choose one of the pseu-

dospin structures

$$\langle \langle \sigma_{\mathbf{t}_n + \mathbf{d}_i}^x, \sigma_{\mathbf{t}_n + \mathbf{d}_i}^y \rangle \rangle = \begin{cases} (0, \langle \sigma^y \rangle) & (i = 0, 3) \\ -(0, \langle \sigma^y \rangle) & (i = 1, 2) \end{cases} \text{ (PAF)} \quad (17)$$

and

$$\langle \langle \sigma_{\mathbf{t}_n + \mathbf{d}_i}^x, \sigma_{\mathbf{t}_n + \mathbf{d}_i}^y \rangle \rangle = (0, \langle \sigma^y \rangle) \quad (i = 0, 1, 2, 3) \text{ (PF)}. \quad (18)$$

We apply the simple linear spin-wave theory, MF-RPA³⁰ (mean field, random phase approximation), in the same way as described in §3.5.2 of Ref. 30. In MF-RPA, $\langle \sigma^y \rangle$ of Eqs. (17) and (18) is calculated by the MF approximation. For the present purpose, we are interested in elementary excitations only at low temperatures, and $\langle \sigma^y \rangle = 1$ is a good approximation. To obtain dispersion relations of pseudospin waves, MF-RPA utilizes the generalized susceptibility $\chi(\mathbf{k}, E)$ and neutron magnetic scattering intensity $S(\mathbf{Q}, E)$ ³⁰. Useful examples of MF-RPA computations including straightforward technical extensions for pyrochlore structures are described Refs. 34 and 35. General computational treatments of MF-RPA are discussed in Refs. 36, and 37. Following these references^{30; 34; 35; 37}, the generalized susceptibility is given by

$$\chi(\mathbf{k}, E) = [1 - \chi^0(E)J(\mathbf{k})]^{-1} \chi^0(E). \quad (19)$$

where \mathbf{k} is a wave vector in the first Brillouin zone, $\chi^0(E)$ and $J(\mathbf{k})$ denote the single-site generalized-susceptibility of the MF Hamiltonian and the Fourier transform of the exchange and dipolar coupling constants. The neutron magnetic scattering intensity $S(\mathbf{Q} = \mathbf{G} + \mathbf{k}, E)$ is given by

$$S(\mathbf{Q}, E) \propto \frac{1}{1 - e^{-\beta E}} \sum_{\rho, \sigma} (\delta_{\rho, \sigma} - \hat{Q}_\rho \hat{Q}_\sigma) \times \sum_{i, i'} U_{\rho, z}^{(i)} U_{\sigma, z}^{(i')} \text{Im} \left\{ \chi_{i, z; i', z}(\mathbf{k}, E) e^{-i\mathbf{G} \cdot (\mathbf{d}_i - \mathbf{d}_{i'})} \right\} \quad (20)$$

where only the local z -component of the pseudospin σ_r^z contribute to the scattering. If one assumes that all the pseudospin components represent a magnetic dipole moment vector with an isotropic g -factor, virtual neutron scattering intensity $S_v(\mathbf{Q}, E)$ is given by

$$S_v(\mathbf{Q}, E) \propto \frac{1}{1 - e^{-\beta E}} \sum_{\rho, \sigma} (\delta_{\rho, \sigma} - \hat{Q}_\rho \hat{Q}_\sigma) \times \sum_{i, \alpha, i', \alpha'} U_{\rho, \alpha}^{(i)} U_{\sigma, \alpha'}^{(i')} \text{Im} \left\{ \chi_{i, \alpha; i', \alpha'}(\mathbf{k}, E) e^{-i\mathbf{G} \cdot (\mathbf{d}_i - \mathbf{d}_{i'})} \right\} \quad (21)$$

where $U_{\rho,\alpha}^{(i)}$ is the rotation matrix^{34; 35} from the local (α) frame defined at the sites $\mathbf{t}_n + \mathbf{d}_i$ to the global (ρ) frame. $S_v(\mathbf{Q}, E)$ is useful when displaying dispersion relations of all pseudospin waves, because the amplitude of the electric quadrupole moment are excluded for $S(\mathbf{Q}, E)$.

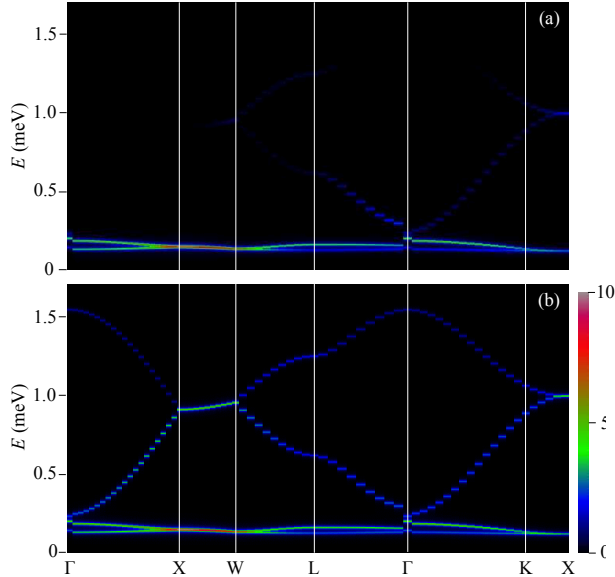


Fig. 1. Magnetic $S(\mathbf{Q}, E)$ (a) and virtual $S_v(\mathbf{Q}, E)$ (b) of the PAF ordering (Eq. (17)) using interaction parameters $J_{nn} = 1$ K, $q = 0.85$, and $\delta = 0$.

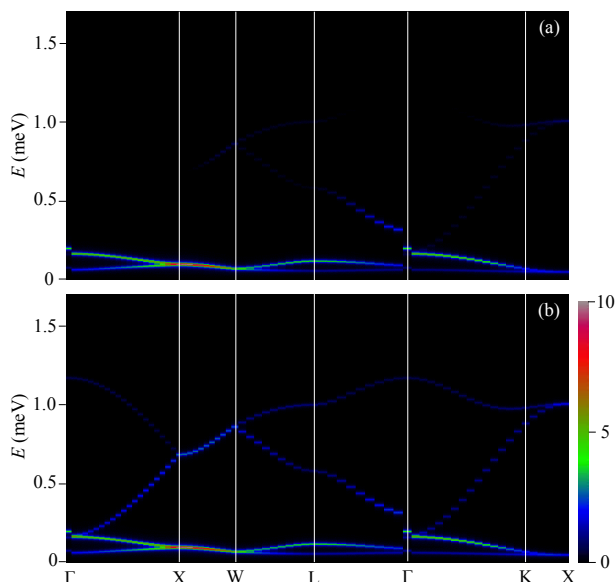


Fig. 2. Magnetic $S(\mathbf{Q}, E)$ (a) and virtual $S_v(\mathbf{Q}, E)$ (b) of the PAF ordering (Eq. (17)) using interaction parameters $J_{nn} = 1$ K, $q = 0.5$, and $\delta = 0.6$.

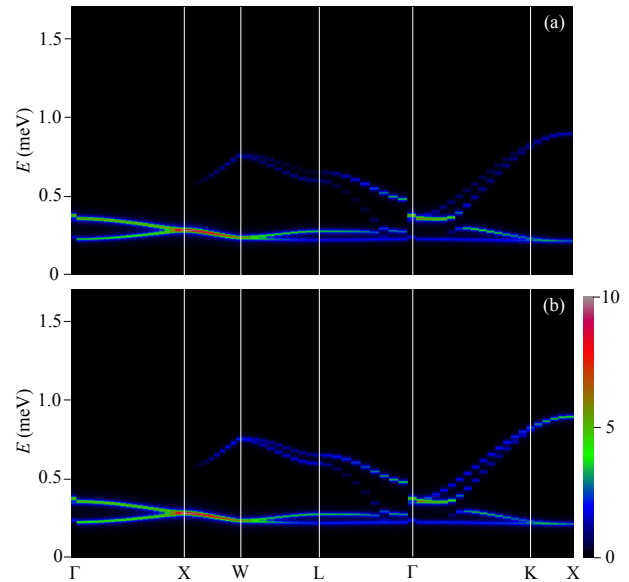


Fig. 3. Magnetic $S(\mathbf{Q}, E)$ (a) and virtual $S_v(\mathbf{Q}, E)$ (b) of the PF ordering (Eq. (18)) using interaction parameters $J_{nn} = 1$ K, $q = 0.8$, and $\delta = -0.6$.

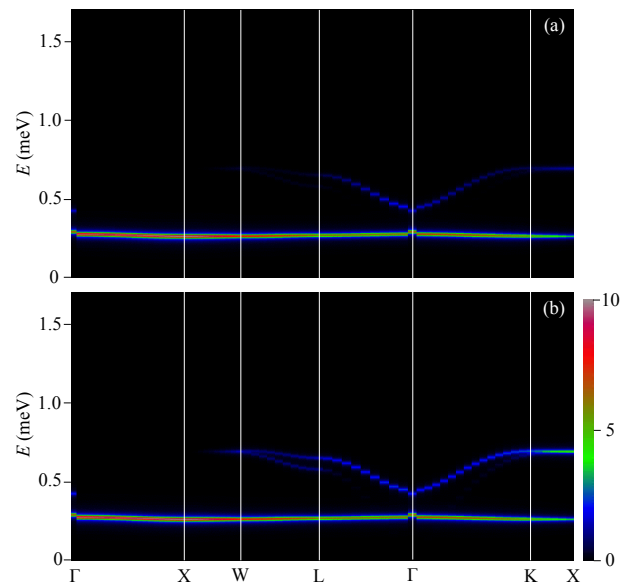


Fig. 4. Magnetic $S(\mathbf{Q}, E)$ (a) and virtual $S_v(\mathbf{Q}, E)$ (b) of the PF ordering (Eq. (18)) using interaction parameters $J_{nn} = 1$ K, $q = 0$, and $\delta = -0.6$.

In Fig. 1(a) we show the inelastic magnetic scattering intensity $S(\mathbf{Q}, E)$ (Eq. (20)) of the the PAF ordering (Eq. (17)) along several symmetry directions in the FCC Brillouin zone using the interaction parameters $J_{nn} = 1$ K, $q = 0.85$, and $\delta = 0$ adopted in Ref. 23. One can see two flat excitation branches in Fig. 1(a). We also show the virtual $S_v(\mathbf{Q}, E)$ (Eq. (21)) in Fig. 1(b). This figure clearly shows that there are four excitation branches consistent with the $\mathbf{k} = 0$ structure possessing four

sites in the unit cell. These four pseudospin-wave branches are composite spin (σ_r^z) and quadrupole (σ_r^x) waves. Figs. 1(a) and (b) show that the amplitude of the spin components is strong and weak in the two lower- E and the two higher- E branches, respectively. Fig. 2 shows the magnetic $S(\mathbf{Q}, E)$ and virtual $S_v(\mathbf{Q}, E)$ using different parameters $J_{\text{nn}} = 1$ K, $q = 0.5$, and $\delta = 0.6$ in the PAF phase (Eq. (17)). The two lower- E excitation branches become more dispersive by the finite value of δ compared to Fig. 1.

In Fig. 3 we show the magnetic $S(\mathbf{Q}, E)$ and virtual $S_v(\mathbf{Q}, E)$ using parameters $J_{\text{nn}} = 1$ K, $q = 0.8$, and $\delta = -0.6$, which are in the PF phase (Eq. (18)). Compared to the PAF cases, the difference between the magnetic and virtual $S(\mathbf{Q}, E)$ becomes less pronounced. Fig. 4 shows the magnetic $S(\mathbf{Q}, E)$ and virtual $S_v(\mathbf{Q}, E)$ using parameters $J_{\text{nn}} = 1$ K, $q = 0$, and $\delta = -0.6$ in the PF phase (Eq. (18)). For vanishing $q = 0$, the two lower- E branches are more flattened and merge into almost one branch.

5. Magnetic Spectra of Polycrystalline $\text{Tb}_{2+x}\text{Ti}_{2-x}\text{O}_{7+y}$

Finally, we would like to compare the previously observed¹⁶ inelastic magnetic neutron scattering spectra peaked around $E = 0.1$ meV with the present pseudospin wave calculation. The sample is the polycrystalline $\text{Tb}_{2+x}\text{Ti}_{2-x}\text{O}_{7+y}$ with $x = 0.005$ ($T_c = 0.5$ K)¹⁶. The neutron scattering experiment was performed on the time-of-flight spectrometer ILL-IN5 operated with $\lambda = 10$ Å. Fig. 5(b) shows Q -dependent powder spectra taken at $T = 0.1$ K. These data should be compared with powder averaging of the magnetic $S(\mathbf{Q}, E)$. Fig. 5(a) shows an example of this powder averaged $S(|\mathbf{Q}|, E)$ choosing the parameters $J_{\text{nn}} = 1$ K, $q = 0.8$, and $\delta = 0$, which are in the PAF phase (Eq. (17)). We think that these figures show reasonably good agreement between the calculation and the observation. In spite of using the over-simplified model Hamiltonian for TTO and the crude linear-spin-wave theory for the frustrated quantum system, essential features of experimental spectra can be reproduced by the approximate calculation. The slight Q -dependence and the non-resolution limited peak-width, $\Delta E \gg (\Delta E)_{\text{resolution}} = 0.01$ meV, have been one of the puzzling observations of TTO. The present interpretation using the composite spin-quadrupole wave can be an answer²³.

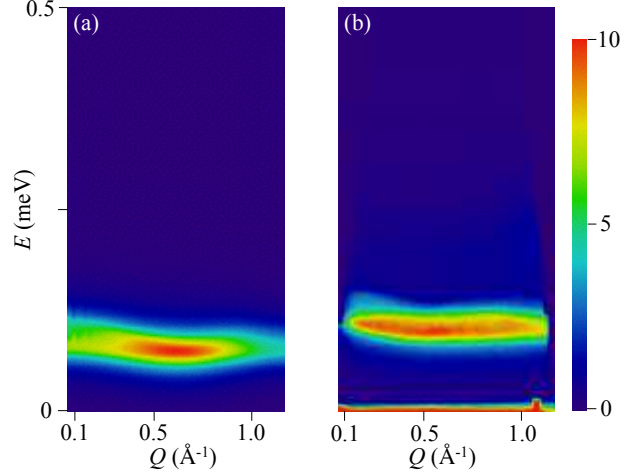


Fig. 5. (a) Powder averaged magnetic $S(|\mathbf{Q}|, E)$ of the PAF ordering (Eq. (17)) using interaction parameters $J_{\text{nn}} = 1$ K, $q = 0.8$, and $\delta = 0$. (b) Inelastic neutron scattering spectra of polycrystalline $\text{Tb}_{2+x}\text{Ti}_{2-x}\text{O}_{7+y}$ with $x = 0.005$ at $T = 0.1$ K well below T_c .

6. Summary

In this study, we try to reformulate the problem of $\text{Tb}_{2+x}\text{Ti}_{2-x}\text{O}_{7+y}$ and reinterpret its puzzling experimental facts based on the theoretically predicted²⁴ pseudospin-1/2 Hamiltonian including the electronic superexchange interaction between electric quadrupole moments. In this scenario, the hidden order in some TTO samples is an electric quadrupolar LRO. Although this LRO does not give rise to strong magnetic Bragg scattering, it can be observed by inelastic magnetic neutron scattering as a composite spin-quadrupole wave. We employ a MF-RPA linear spin-wave theory and compare its computation with previously observed low-energy magnetic excitation spectra of a polycrystalline sample with $x = 0.005$ ($T_c = 0.5$ K). Quite intriguingly, the interaction parameters used in Fig. 5(a) are located very close to the phase boundary between the PAF and U(1) quantum spin-liquid states^{7; 24; 23}. This may possibly imply that $\text{Tb}_{2+x}\text{Ti}_{2-x}\text{O}_{7+y}$ samples with $x < x_c$ are in the U(1) quantum spin-liquid phase²³.

Acknowledgments

We thank S. Onoda and Y. Kato for useful discussions. This work was supported by JSPS KAKENHI grant numbers 25400345 and 26400336. The neutron scattering performed using ILL-IN5 (France) was transferred from JRR3-HER (proposal 11567) with the approval of ISSP, Univ. of Tokyo, and

JAEA, Tokai, Japan.

References

1. C. Lacroix, P. Mendels and F. Mila (eds.), *Introduction to Frustrated Magnetism* (Springer, Berlin, Heidelberg, 2011).
2. J. S. Gardner, M. J. P. Gingras and J. E. Greedan, *Rev. Mod. Phys.* **82**, 53 (2010).
3. S. T. Bramwell and M. J. P. Gingras, *Science* **294**, 1495 (2001).
4. C. Castelnovo, R. Moessner and S. L. Sondhi, *Nature* **451**, 42 (2008).
5. M. Hermele, M. P. A. Fisher and L. Balents, *Phys. Rev. B* **69**, 064404 (2004).
6. L. Savary and L. Balents, *Phys. Rev. Lett.* **108**, 037202 (2012).
7. S. Lee, S. Onoda and L. Balents, *Phys. Rev. B* **86**, 104412 (2012).
8. Y. Kato and S. Onoda, arXiv:1411.1918.
9. M. J. P. Gingras and P. A. McClarty, *Rep. Prog. Phys.* **77**, 056501 (2014).
10. O. Benton, O. Sikora and N. Shannon, *Phys. Rev. B* **86**, 075154 (2012).
11. L.-J. Chang, S. Onoda, Y. Su, Y.-J. Kao, K.-D. Tsuei, Y. Yasui, K. Kakurai and M. R. Lees, *Nature Communications* **3**, 992 (2012).
12. K. A. Ross, L. Savary, B. D. Gaulin and L. Balents, *Phys. Rev. X* **1**, 021002 (2011).
13. J. S. Gardner, S. R. Dunsiger, B. D. Gaulin, M. J. P. Gingras, J. E. Greedan, R. F. Kiefl, M. D. Lumsden, W. A. MacFarlane, N. P. Raju, J. E. Sonier, I. Swainson and Z. Tun, *Phys. Rev. Lett.* **82**, 1012 (1999).
14. H. R. Molavian, M. J. P. Gingras and B. Canals, *Phys. Rev. Lett.* **98**, 157204 (2007).
15. H. Takatsu, H. Kadowaki, T. J. Sato, J. W. Lynn, Y. Tabata, T. Yamazaki and K. Matsuhira, *J. Phys. Condens. Matter* **24**, 052201 (2012).
16. T. Taniguchi, H. Kadowaki, H. Takatsu, B. Fåk, J. Ollivier, T. Yamazaki, T. J. Sato, H. Yoshizawa, Y. Shimura, T. Sakakibara, T. Hong, K. Goto, L. R. Yaraskavitch and J. B. Kycia, *Phys. Rev. B* **87**, 060408 (2013).
17. S. Petit, P. Bonville, J. Robert, C. Decorse and I. Mirebeau, *Phys. Rev. B* **86**, 174403 (2012).
18. T. Fennell, M. Kenzelmann, B. Roessli, H. Mutka, J. Ollivier, M. Ruminy, U. Stuhr, O. Zaharko, L. Bovo, A. Cervellino, K. Haas, M. and J. Cava, *R. Phys. Rev. Lett.* **112**, 017203 (2014).
19. K. Fritsch, K. A. Ross, Y. Qiu, J. R. D. Copley, T. Guidi, R. I. Bewley, H. A. Dabkowska and B. D. Gaulin, *Phys. Rev. B* **87**, 094410 (2013).
20. K. Fritsch, E. Kermarrec, K. A. Ross, Y. Qiu, J. R. D. Copley, D. Pomaranski, J. B. Kycia, H. A. Dabkowska and B. D. Gaulin, *Phys. Rev. B* **90**, 014429 (2014).
21. S. Petit, S. Guitteny, J. Robert, P. Bonville, C. Decorse, J. Ollivier, H. Mutka and I. Mirebeau, *EPJ Web of Conferences* **83**, 03012 (2015).
22. Y. Chapuis, Ph.D. thesis, Université Joseph Fourier (2009), <http://tel.archives-ouvertes.fr/tel-00463643/en/>.
23. H. Takatsu, S. Kittaka, A. Kasahara, Y. Kono, T. Sakakibara, Y. Kato, S. Onoda, B. Fåk, J. Ollivier, J. W. Lynn, T. Taniguchi, M. Wakita, and H. Kadowaki, arXiv:1506.04545.
24. S. Onoda and Y. Tanaka, *Phys. Rev. B* **83**, 094411 (2011).
25. M. J. P. Gingras, B. C. den Hertog, M. Faucher, J. S. Gardner, S. R. Dunsiger, L. J. Chang, B. D. Gaulin, N. P. Raju and J. E. Greedan, *Phys. Rev. B* **62**, 6496 (2000).
26. I. Mirebeau, P. Bonville and M. Hennion, *Phys. Rev. B* **76**, 184436 (2007).
27. A. Bertin, Y. Chapuis, P. Dalmas de Réotier and A. Yaouanc, *J. Phys. Condens. Matter* **24**, 256003 (2012).
28. J. Zhang, K. Fritsch, Z. Hao, B. V. Bagheri, M. J. P. Gingras, G. E. Granroth, P. Jiramongkolchai, R. J. Cava and B. D. Gaulin, *Phys. Rev. B* **89**, 134410 (2014).
29. A. J. Princep, H. C. Walker, D. T. Adroja, D. Prabhakaran and A. T. Boothroyd, arXiv:1501.04927.
30. J. Jensen and A. R. Mackintosh, *Rare Earth Magnetism* (Clarendon Press, Oxford, 1991).
31. H. Kusunose, *J. Phys. Soc. Jpn.* **77**, 064710 (2008).
32. B. C. den Hertog and M. J. P. Gingras, *Phys. Rev. Lett.* **84**, 3430 (2000).
33. S. V. Isakov, R. Moessner and S. L. Sondhi, *Phys. Rev. Lett.* **95**, 217201 (2005).
34. Y.-J. Kao, M. Enjalran, A. Del Maestro, H. R. Molavian and M. J. P. Gingras, *Phys. Rev. B* **68**, 172407 (2003).
35. S. Petit, P. Bonville, I. Mirebeau, H. Mutka and J. Robert, *Phys. Rev. B* **85**, 054428 (2012).
36. M. Rotter, *Comput. Mater. Sci.* **38**, 400 (2006).
37. M. Rotter et al., Manual and references of McPhase, <http://www.mcphase.de/>.